EASR

Engineering and Applied Science Research

https://www.tci-thaijo.org/index.php/easr/index

Published by the Faculty of Engineering, Khon Kaen University, Thailand

Optimization process for enhancing the recovery of ammonium and phosphate from wastewater by modified rice husk biochar

Nguyen Lan Thanh[1, 2)], Nguyen Le Huong Nguyet[1, 2)], Van Giang Le[3)], Nguyen Thi Thuy[2, 4)], Vo Hoang Nhat Phong[5)], Vo Nguyen Xuan Que[1, 2)], Vo Thanh Hang[1, 2)] and Nguyen Nhat Huy*[1, 2)]

[1)]Faculty of Environment and Natural Resources, Ho Chi Minh City University of Technology (HCMUT), Ho Chi Minh City, Vietnam
[2)]Vietnam National University Ho Chi Minh City, Ho Chi Minh City, Vietnam
[3)]Central Institute for Natural Resources and Environmental Studies, Vietnam National University, Hanoi, Vietnam
[4)]School of Chemical and Environmental Engineering, International University, Ho Chi Minh City, Vietnam
[5)]School of Chemical Engineering, The University of Queensland, St. Lucia 4072, Queensland, Australia

Received 31 August 2022
Revised 3 March 2023
Accepted 22 March 2023

Abstract

This study aimed to optimize the recovery of ammonium and phosphate from wastewater using Mg-modified biochar as an adsorbent. Given the situation of domestic wastewater and agricultural waste in Vietnam, the researchers fabricated biochar from rice husk and modified it with magnesium salt to make it an effective material for wastewater treatment. To determine the optimal conditions for the experiments, the response surface methodology was used, specifically the central composite design (CCD) model with four factors, namely biochar dosage (g/L), pH, N:P ratio, and initial concentrations of NH_4^+ and PO_4^{3-}. The material was thoroughly characterized using scanning electron microscopy (SEM), Fourier-transform infrared spectroscopy (FTIR), energy-dispersive X-ray spectroscopy (EDS), and X-ray diffraction (XRD) to ensure that it met the desired specifications. Based on the experimental design, the optimal conditions were determined to be a biochar dosage of 0.12 g/L, an N:P ratio of 1.25, an initial concentration of 60 mg/L, and a pH of 6. Tests conducted in synthetic wastewater produced results that were in agreement with the predicted values. However, when the optimized values were tested in domestic wastewater, only phosphate removal showed good agreement with an efficiency of 93% compared to the predicted optimization value of 88%. This study demonstrates the potential of Mg-modified biochar as an effective adsorbent for recovering ammonium and phosphate from wastewater. Although further optimization may be required for ammonium removal in domestic wastewater, the results are promising and warrant further investigation.

Keywords: Biochar, Ammonia, Phosphate, Adsorption, Rice husk

1. Introduction

Vietnam's economy heavily relies on agriculture, and after joining the World Trade Organization, investments in the industry have increased [1]. However, this has resulted in a rise in agricultural waste. Annually, the country disposes of 6.8 million tons of rice husk, 5.8 million tons of sawdust, and 0.3 to 0.5 million tons of coffee leftovers during the harvesting and processing of agricultural products [2]. In a recent report, it was noted that 40.8 million tons of rice husks and straw, 15.6 million tons of leaves and sugarcane refuse, 9.2 million tons of cobs, 1.17 million tons of coffee husk, and 1.12 million tons of sawdust are produced each year [3]. Despite the huge potential for recycling this agricultural waste, only a small amount is being utilized. For example, only 10% is used as fuel in brick kilns and rural households, 5% as industrial fuel (e.g., rice husk and bagasse), and 3% for feeding cattle and fertilizer production. The remaining 80% is discharged into canals, rivers, or burned, which poses a significant threat of water and air pollution [4, 5]. It is noteworthy that rice husk is the most abundant type of crop residue, particularly in the Mekong Delta of Vietnam [6]. Addressing this waste management issue would not only benefit the environment but could also provide valuable resources for various industries. Therefore, it is crucial to develop effective and sustainable approaches to utilize agricultural waste and prevent further pollution.

Biochar, a product that can be derived from agricultural waste [7, 8], is a promising solution to increase crop yield by improving soil quality. It helps maintain and stabilize moisture, fertilizer, and soil microorganisms [9-12]. Additionally, biochar is an excellent adsorbent for removing various environmental contaminants. Untreated wastewater discharge is currently a significant environmental concern due to its high concentrations of nutrients [13, 14], particularly nitrogen and phosphorus, which cause eutrophication - algal bloom and subsequent oxygen depletion - in receiving water bodies [15-17]. Various environmental technologies have attempted to address eutrophication [18-20], but adsorption remains a reliable and cost-effective technology for removing metals and nutrients [17, 21-24]. Using biochar as an adsorbent for removing nutrients in wastewater is, therefore, a viable solution to reducing agricultural waste and mitigating eutrophication concerns [25-27]. By utilizing biochar, we can reduce the amount of agricultural waste discharged and enhance the quality of water bodies. This will not only benefit the environment but also contribute to the sustainable development of agriculture in Vietnam. In addition, the amount of minable phosphorous in the world is finite and not evenly distributed, which poses

*Corresponding author.
Email address: nnhuy@hcmut.edu.vn
doi: 10.14456/easr.2023.20

a challenge to sustainable agricultural practices. Despite some studies suggesting otherwise, it is estimated that the global commercial supply of phosphorous for agricultural use will be depleted within the next century and cannot be replaced [28]. At the same time, the demand for phosphorous is increasing by 2.5% annually, and by 2035, it is projected to exceed the available supply worldwide [29]. In addition, nitrogen is a crucial element for life, and while biological nitrogen fixation can provide an adequate amount of N_2, it is not fast enough to meet the global nitrogen demands for crops [29]. The worldwide nitrogen challenge is to maximize the net positive impact of commercial nitrogen fertilizers, both inorganic and organic, on human health, the environment, and economic well-being [30]. Although animal manure and legumes can partially fulfill the N requirements for agricultural production, they are insufficient to meet the needs of current and future generations [30]. Therefore, to satisfy the growing demand for N and P in agricultural production and prevent the eutrophication of wastewater, the recovery of N and P should be a priority shortly.

Optimizing analytical processes is crucial in research and development, and testing plays a key role in this [31, 32]. The most employed optimization approach involves investigating each factor separately, also known as the one-factor-at-a-time approach. However, this method has limitations because multiple factors may influence the findings simultaneously, and the final conditions may not be the best ones [32, 33]. To address this, a viable and widely used option is the response surface methodology (RSM) combined with a central composite design (CCD) [34]. This statistical technique considers the interactions among variables and depicts the cumulative effects of factors on the process [35], making it more practical than traditional experimental methods [36]. Many studies have successfully employed RSM to optimize their experiments, including those on field pea Shiro flour [31], biodiesel production [35], fluoride adsorption [37], norfloxacin adsorption with coffee ground biochar [38], and copper removal using lobster shell biochar [39].

According to the situation in Vietnam and the idea from previous research, the study is to solve three problems, including (i) domestic wastewater, (ii) reducing the experimental time, and (iii) agricultural waste. The Mg-biochar was used to remove phosphate (PO_4^{3-}) and ammonium (NH_4^+) from wastewater following the standard (National technical regulation on domestic wastewater, QCVN 14:2008/BTNMT). A CCD model was used to optimize the experimental design, thus reducing the number of conducted experiments. Real wastewater collected from a household (domestic wastewater) was also used to test the performance of the biochar.

2. Materials and methods

2.1 Biochar preparation

Rice husk was first dried overnight at 55 °C. Then, 10 g of dried rice husk was mixed with 200 mL of 10% $MgCl_2$ solution in a 500-mL Erlenmeyer shaken at 120 rpm for 24 h. After $MgCl_2$ permeated fully into the rice husk, the product was dried at 80 °C until no water was observed. It was further dried at 106 °C for 6 h. Next, the product was heated at 550 °C in an oven for 1 h to produce biochar, which was stored in a desiccator before use. Biochar was then characterized by Fourier transform infrared spectroscopy (FTIR, Iraffinity-1, Shimadzu, Japan), energy-dispersive X-ray spectroscopy (EDS, EMSA/MAS Spectral Data File, Japan), scanning electron microscopy (SEM, S-4800, Hitachi, Japan), and X-ray diffraction (XRD, D8 Advance, Bruker, Germany). The overall process of biochar fabrication and adsorption experiment with synthetic or actual wastewater is shown in Figure 1.

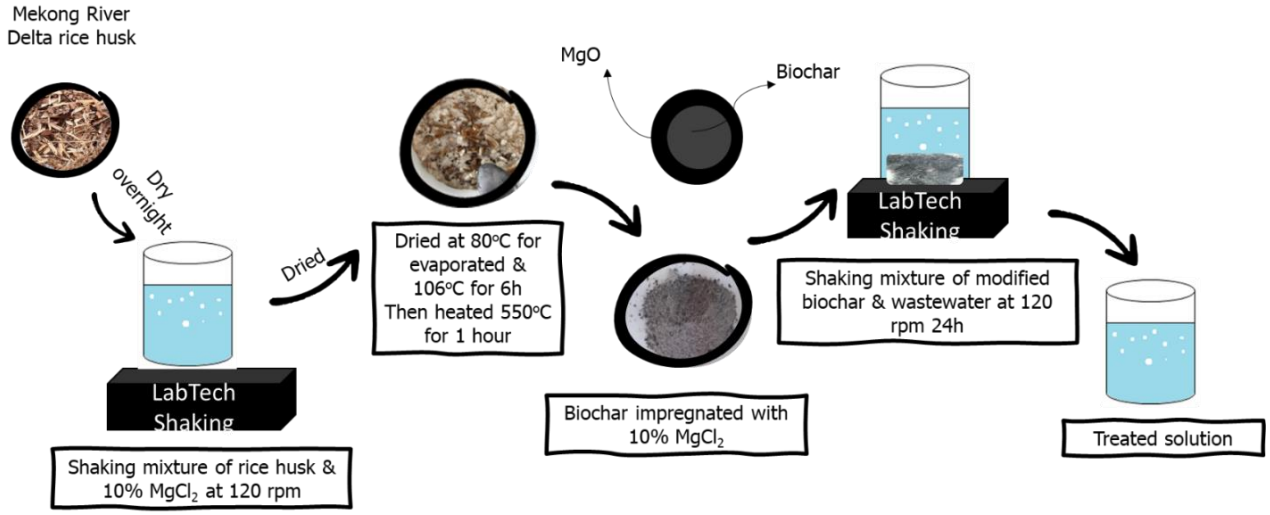

Figure 1 Schematic of modified biochar fabricating process and nutrient recovery application

2.2 Adsorption experiment

Synthetic wastewater was made with 30 – 70 mg/L of NH_4^+ and PO_4^{3-} from NH_4Cl and KH_2PO_4 salts, respectively, with a ratio of NH_4^+ and PO_4^{3-} (denoted as N:P ratio) of 0.5 – 1.5 and pH 5 – 9. Biochar with an amount of 0.06 – 0.12 g was added into 100 mL of synthetic wastewater and shaken at 120 rpm for 24 h. Collected samples were paper-filtered (Newstar 102, Φ 110 mm) and analyzed for PO_4^{3-} (TCVN 6202:2008 with spectrophotometer DR5000 at 690 nm wavelength) and NH_4^+ (TCVN 5988:1995 – distillation method and titration with Buchi distillation unit K-355).

The nutrient removal efficiency of biochar is calculated based on the following equation:

$$H = ((C_{in} - C_{out})/C_{in})*100 \quad (1)$$

Where H is the adsorption efficiency (%). C_{in} and C_{out} are initial and final nutrient concentrations (mg/L).

2.3 Central composite design modeling

The RSM of CCD [40, 41] can provide constant prediction variance at all points [32]. CCD is built on a factorial design and adds a center point and axial points [42]. The CCD in this study consisted of four different factors, namely (A) biochar dosage (mg/L), (B) initial concentrations of PO_4^{3-} (mg/L), (C) N:P ratio, and (D) pH. The design involved 2^k factorial points enlarged by a center point and 2k axial points (number of factors is k). The codes of four variables (A, B, C, and D) were organized at five stages, namely: minimum, -1, 0 (central), +1, and maximum. These five levels were assessed based on a face-centered CCD experimental plan. The experimental design is shown in Table 1 while the results are given in Table 2.

Table 1 Central composite design's experimental design

Codes	Factors	Units	Min	Max	Coded Low	Coded High	Mean	S. D
A	Biochar dosage	mg/L	60	140	-1 ↔ 80	+1 ↔ 120	100	18.19
B	Initial concentration	mg/L	30	70	-1 ↔ 40	+1 ↔ 60	50	9.10
C	N:P		0.5	1.5	-1 ↔ 0.75	+1 ↔ 1.25	1	0.2274
D	pH		5	9	-1 ↔ 6	+1 ↔ 8	7	0.9097

Table 2 Results of central composite design's experiments

Run	A	B	C	D	NH_4^+ H%	q_e mg/g	PO_4^{3-} H%	q_e mg/g
1	120	60	0.75	8	89.72	32.60	93.20	47.76
2	100	50	1	7	85.81	38.62	76.87	34.75
3	140	50	1	7	86.31	27.74	91.15	29.43
4	100	30	1	7	84.00	23.52	85.46	13.34
5	60	50	1	7	59.56	50.03	49.30	37.14
6	80	60	0.75	8	62.75	34.20	82.58	63.47
7	120	60	0.75	6	88.95	32.32	88.64	33.25
8	120	60	1.25	6	81.84	50.47	86.17	43.42
9	80	40	0.75	6	68.00	23.80	80.93	35.95
10	120	60	1.25	8	81.84	50.47	88.94	35.53
11	80	40	1.25	8	82.08	51.30	83.46	31.77
12	100	50	1	7	70.00	35.28	85.62	38.70
13	100	50	1	5	85.44	42.72	76.25	35.59
14	80	60	1.25	8	76.11	71.35	86.88	52.07
15	100	50	1	9	95.52	47.76	93.13	37.82
16	100	50	1	7	88.13	44.06	75.65	31.98
17	100	50	1.5	7	86.56	64.92	83.38	37.69
18	100	50	1	7	83.86	39.00	82.21	30.42
19	80	60	1.25	6	62.67	58.75	80.52	60.87
20	100	50	1	7	85.44	42.72	84.59	31.30
21	120	40	1.25	8	88.80	37.00	94.32	23.94
22	80	40	0.75	8	60.00	21.00	69.63	27.95
23	100	50	0.5	7	66.50	14.90	95.76	40.48
24	120	40	0.75	8	48.00	11.20	90.38	36.28
25	100	70	1	7	76.00	53.20	82.94	56.70
26	100	50	1	7	82.08	41.04	81.42	30.13
27	120	40	1.25	6	93.28	38.87	94.18	29.12
28	80	40	1.25	6	86.56	54.10	78.02	36.18
29	80	60	0.75	6	78.17	42.60	61.52	34.61
30	120	40	0.75	6	60.00	14.00	91.76	27.17

3. Results and discussion

3.1 Biochar's properties

The SEM images revealed that the biochar produced from rice husk had a rough and porous surface [43, 44]. The surface texture was a result of the deposition of MgO flakes on the rice husk's surface, which facilitated the uptake of metals (Figures 2a and 2b). The EDS analysis (Figure 2c) indicated that the produced biochar contained C (14.79%), O (51.41%), Si (8.33%), Mg (16.25%), and Cl (9.22%). In comparison to the work of Li et al. [18], the Mg content (23.94%) in their 20% Mg-biochar was higher than that in our study for 10% Mg-biochar, and the MgO flakes on the biochar's surface promoted pore formation. Although $MgCl_2$ addition did not influence the enhancement of C% [45], it is known that various salts and mineral deposits have different heat transfer characteristics that affect their contact with the carbonation process during pyrolysis, and thus the pore formation and carbon storage in biochar [18, 46]. The Mg content in this study was consistent with the initial dose (from salt) in the biochar. The O/C and H/C ratios tend to decline with the improvement of heating temperature and time [47]. Typically, biochar is recognized as an OC-rich substance, and thus our study's Mg-biochar was successfully synthesized with an OC content of 760.35 mg/g, comparable to cellulosic biochar (804 mg/g) and rye grass biochar (488 mg/g) [47]. Additionally, the O/C molar ratio of the biochar was 2.6 in this study, which was higher than 0.6, indicating a half-life of fewer than 100 years [48]. However, the correlation between the O/C ratio and biochar stability was not strong, as it depended on the feedstock, morphology, and chemical and physical properties [49].

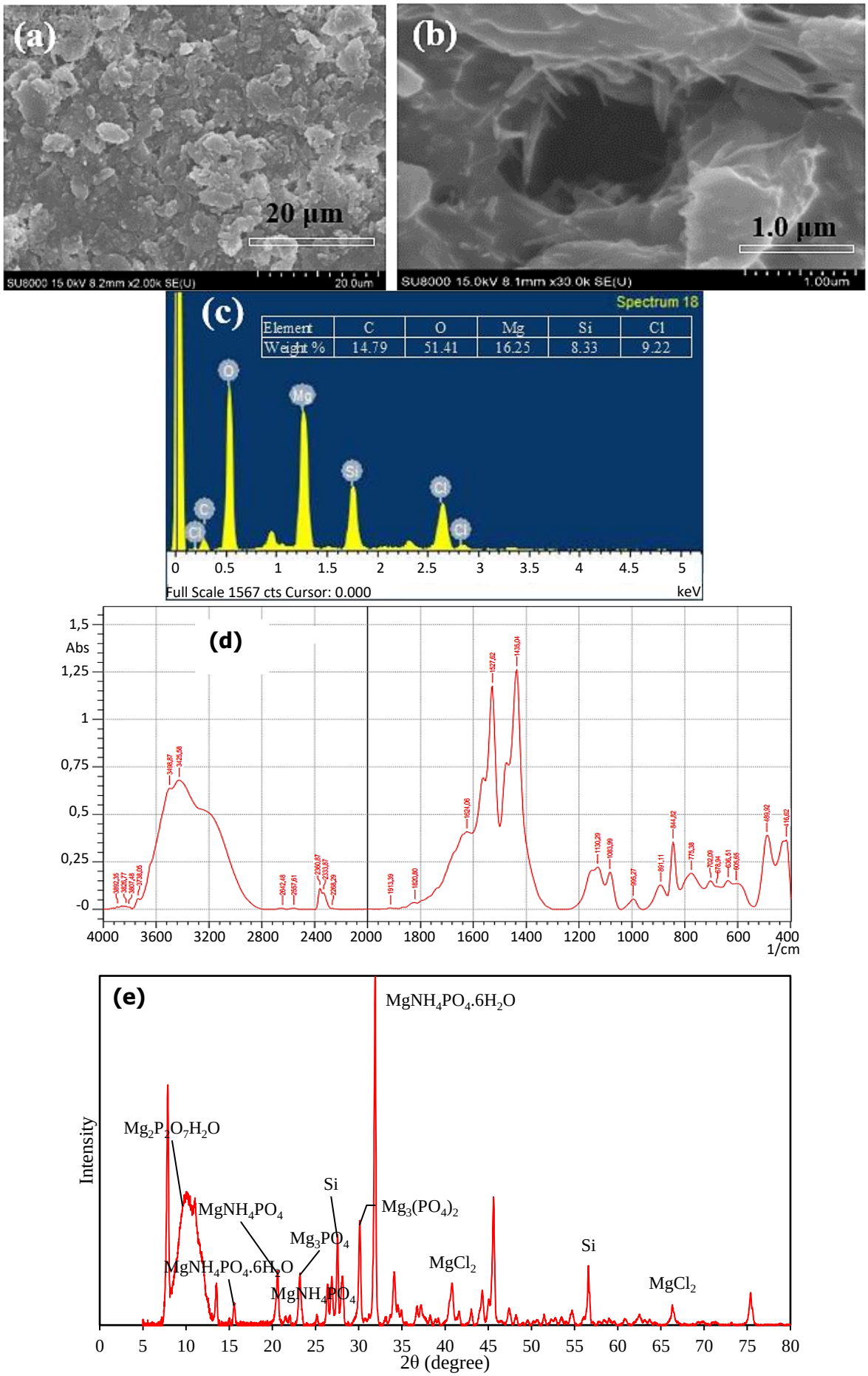

Figure 2 SEM images of (a) ×2000 magnification, scale bar = 20 µm and (b) ×30000 magnification, scale bar = 1 µm, (c) EDS spectrum, and (d) FTIR spectrum of 10% Mg-biochar; and (e) XRD pattern of 10% Mg-biochar after adsorption

Figure 2d shows the FTIR spectrum of the biochar. The peaks around 416.62 – 678.94 cm^{-1} were Si-O bending strength vibrations of the SiO_2 [50]. While both Si-O and C=O bending vibrations of CO_2 were related to the peaks at 702.09 cm^{-1} and 775.38 cm^{-1}, respectively [51]. The peak at 995.27 cm^{-1} was assigned to the Si-O stretching vibration. The peaks at 1038.99 cm^{-1} and 1435.04 cm^{-1} showed the appearance of C-N single bond and C=N covalent bond stretching vibrations, respectively, whereas the peak at 1130.29 cm^{-1} was the CH_3 group symmetric vibration. The peaks at 1527.62 – 1624.06 cm^{-1} were the benzene ring C=C of aromatic compounds. The presence of a C=C double bond in the molecule could potentially affect its polarity and subsequently impact its interaction with ammonium ions [8, 52]. Additionally, the polar nature of the carbonyl group may promote the adsorption of ammonium ions. Furthermore, the C=C double bond can alter the molecule's steric and electrical characteristics, ultimately affecting its ability to adsorb ammonium ions [8, 52]. The appearance of two significant peaks at 3425.58 cm^{-1} and 3498.87 cm^{-1} indicated the Mg-OH stretching vibration. The appearance of a strong asymmetric P-O bond vibration peak at 1083 cm^{-1} suggested that PO_4^{3-} was effectively absorbed onto the metal oxide surface of Mg-O by forming an inner-sphere surface complex [53, 54]. The peaks at 3807.48 – 3892.36 cm^{-1} demonstrated the presence of OH stretching vibration of adsorbed water or hydroxyl group [51]. It is believed that the adsorbed ammonium ion may react with the hydroxyl group through hydrogen bonding, decreasing the -OH bond energy [53]. Additionally, the presence of OH- is thought to enhance the biochar's ability to adsorb ammonium ions due to electrostatic attraction [11, 19, 29, 53]. However, the presence of a broad peak at 1083.99 cm^{-1}, with a clear peak at 1130.29 cm^{-1}, suggests the existence of certain out-sphere interface complexes such as $H_2PO_4^-$ [54, 55]. The positively charged MgO flake on the surface may preferentially attract this form of phosphate through electron attraction [54, 55].

Figure 2e displays the XRD pattern of 10% Mg-biochar after being successfully applied in synthesizing wastewater. The peaks at 2θ approximately 40.8° and 66.38° signified the presence of magnesium chloride ($MgCl_2$) [2, 8, 18, 47], indicating the successful modification of Mg on the biochar surface. The peaks at 2θ of 56.6° and 23.2° corresponded to Si, which aligned with the EDS results. By maintaining a proportion of 1:1:1 for ammonium, phosphate, and magnesium in an alkaline environment, struvite ($MgNH_4PO_4$, MAP) precipitation could take place [13, 14]. The sturdy peaks of struvite ($MgNH_4PO_4$ and $MgNH_4PO_4.6H_2O$) were found at 2θ of 20.68°, 25.67°, and 15.8°, substantiating the precipitation among ammonium, phosphate, and magnesium, resulting in struvite formation [56]. Moreover, peaks at 2θ around 23.11° and 30.16° for $Mg_3(PO_4)_2$ [13, 20, 22] suggested the precipitation between phosphate and magnesium, unveiling that biochar surfaces could adsorb phosphate better than ammonium.

3.2 Central composite design

The fitting of CCD and experimental runs was evaluated by analysis of variance (ANOVA). ANOVA results are shown in Tables 3 and 4. The application of ANOVA technique was utilized to ascertain the significance of the coefficients and the suitability of the proposed model. The P-values were used to determine the significance or insignificance of each coefficient. A P-value less than 0.05 indicated that there was a statistically significant difference between the means. To simplify the model, insignificant terms were removed. Tables 3 and 4 presents the variables before elimination, which were observed through the probability (P-value of each factor). If the model contained several significant terms (excluding those necessary to support the hierarchy), model reduction could improve the model. The final regression equation briefly described the significant value. To enhance the model's performance, further analyses could be conducted. The significant value was briefly described in the final regression equation below.

Table 3 ANOVA of Central composite design and experimental runs

Model variables		**A**	**B**	**C**	**D**
Coefficient estimaste	NH_4^+ removal	4.567	0.8052	5.74	
	q_e, mg/g	-5.61	7.54	12.53	0.1789
	PO_4^{3-} removal	7.82	-0.8033	0.3789	2.56
	q_e, mg/g	-3.41	8.72	0.0364	0.9453
P-value	NH_4^+ removal	0.0093	0.6228	0.0016	
	q_e, mg/g	< 0.0001	< 0.0001	< 0.0001	0.8166
	PO_4^{3-} removal	< 0.0001	0.5805	0.7938	0.0865
	q_e, mg/g	0.0099	< 0.0001	0.9764	0.4451

Table 4 ANOVA of CCD and experimental runs in terms of AB, BC, and CD interactions

Model variables		**AB**	**BC**	**CD**
Coefficient estimaste	NH_4^+ removal	4.33	-8.24	
	q_e, mg/g			
	PO_4^{3-} removal			
	q_e, mg/g			- 4.42
P-value	NH_4^+ removal	0.0388	0.0003	
	q_e, mg/g			
	PO_4^{3-} removal			
	q_e, mg/g			0.0067

From Table 5, the 2FI model was significant for NH_4^+ removal efficiency and the adsorption capacity of PO_4^{3-}, while the linear model was acceptable for the adsorption capacity of NH_4^+ and PO_4^{3-} removal efficiency. In NH_4^+ removal, A, C, AB, and BC were significant while in the adsorption capacity of NH_4^+, A, B, and C were significant. In contrast, the P-values of PO_4^{3-} removal and adsorption capacity of PO_4^{3-} were ≤ 0.05, indicating that both models were significant. In the PO_4^{3-} removal, A was significant while in the adsorption capacity of PO_4^{3-}, A, B, and CD were significant factors. The ANOVA technique, a statistical tool commonly used in research, was utilized to determine the model's significance and suitability. In this context, the F values for the NH_4^+ removal and adsorption capacity were 8.59 and 105.25, respectively, highlighting their high level of statistical significance. Conversely, the F values for PO_4^{3-} removal and adsorption capacity were 8.33 and 13.72, respectively, indicating that these models were also significant. The

low probability of such F values occurring due to noise (0.02% and 0.01%) reinforces their validity. The actual and predicted response values demonstrated strong agreement overall, suggesting the model's effectiveness. Additionally, the Adeq.precision measure was employed to evaluate the signal-to-noise ratio by comparing the range of predicted values to the average prediction error. A ratio exceeding 4 is desirable, and the ammonium ion removal efficiency ratio of 13.123 met this criterion, allowing for effective navigation of the design space. Furthermore, the ratios of ammonium equilibrium adsorption capacity, phosphate ion removal, and phosphate adsorption capacity were found to be larger than 4, with values of 33.87, 10.91, and 13.12, respectively. Such ratios can be used to navigate the design space efficiently.

Table 5 Summary of ANOVA of Central composite design and experimental runs

	NH_4^+ removal %	**q_e, mg/g**	**PO_4^{3-} removal %**	**q_e, mg/g**
Type of model	Reduced 2FI model	Linear	Linear	Reduced 2FI model
Significant model terms	A, C, AB, BC	A, B, C	A	A, B, CD
F value	8.59	105.25	8.33	13.72
Prob > F	< 0.0001	< 0.0001	0.0002	< 0.0001
Std.Dev.	7.92	3.74	7.03	5.96
R^2	0.6416	0.9439	0.5712	0.7408
Adj.R^2	0.5669	0.9350	0.5026	0.6868
Mean	78.13	39.65	83.16	36.83
Adeq.precision	8.0325	33.8754	10.9058	13.1226

Figure 3 evaluates the fitting between the actual and predicted response values. In both NH_4^+ and PO_4^{3-} response normal probability plots, all the points lie near the straight line, indicating the satisfactory correlation of the response values. There was no data that had an impact on the normal distribution of errors for the four models. These errors were also independent of each other's [32].

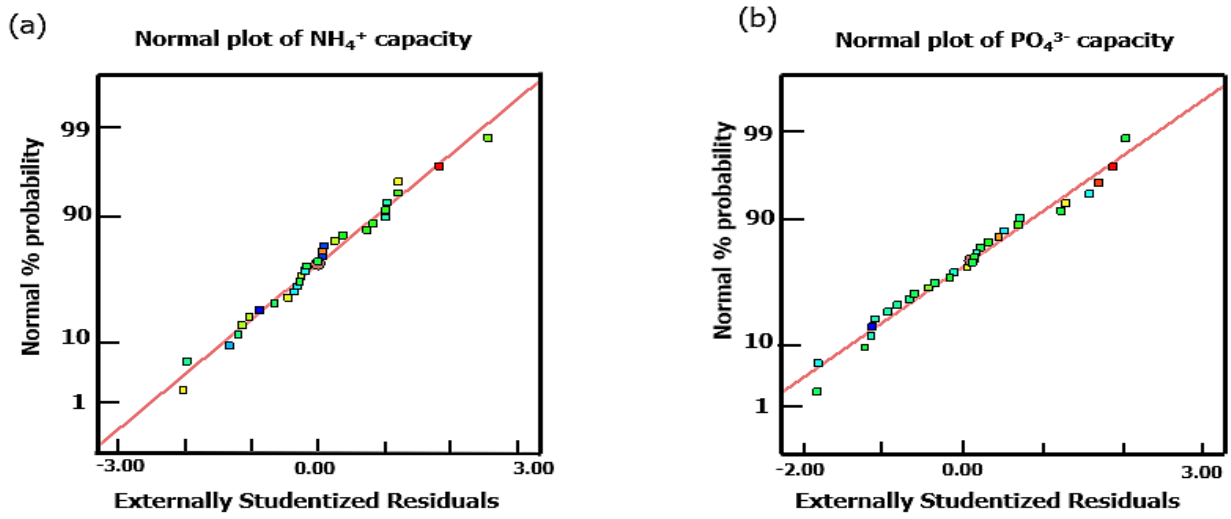

Figure 3 Normal probability plots of residual for (a) NH_4^+ and (b) PO_4^{3-} adsorption capacity

The final regression equations for NH_4^+ and PO_4^{3-} adsorption capacity are as follows:

$$NH_4^+ \text{ adsorption capacity } (q_e, \text{ mg/g}) = 39.65 - 5.61A + 7.54B + 12.53C + 0.1789D \quad (2)$$

$$PO_4^{3-} \text{ adsorption capacity } (q_e, \text{ mg/g}) = 36.83 - 3.41A + 8.72B + 0.0364C + 0.9453D - 4.42CD \quad (3)$$

The three-dimensional surface plots (3D plots) were also used to identify the interrelation between the variables and model response (Figure 4). From Figure 4a, a higher amount of biochar dosage led to a lower capacity of NH_4^+ adsorption. This phenomenon can be explained by the inverse correlation between the amount of adsorbate and adsorbent in the adsorption capacity formula. When the quantity of adsorbent rises with a fixed amount of adsorbate in the solution, the adsorption capacity decreases, albeit the adsorption efficiency rises. Moreover, the heightened utilization of biochar may pose a difficulty for ammonium ions, phosphate ions, and the biochar surface to interact with each other, leading to a contrary trend between them. Furthermore, a slight growth of NH_4^+ adsorption capacity occurred when the initial concentration was from 40 – 60 mg/L. The higher concentration of ammonium ions facilitated better interaction with the negative charge present within the biochar matrix. As evidenced by Figure 4b, an impressive adsorption capacity of NH_4^+ was observed with an increase in the N:P ratio. This was corroborated by the XRD results, which showed that phosphate reacted more readily with Mg to form struvite than with ammonium. Consequently, an increase in the N:P ratio, which corresponded to a higher initial ammonium concentration, was positively correlated with the adsorption capacity of ammonium ions. In contrast to the previous discovery, Figure 4c revealed that the adsorption capacity of PO_4^{3-} was influenced by pH, and an increase in pH from 6 to 8 led to a decrease in PO_4^{3-} adsorption capacity. This decline occurred due to the competition between OH^- and PO_4^{3-} for adsorption sites. It is important to note that the pH level of the solution can impact the adsorption ability of phosphate and the surface properties of biochar [57]. The functional groups present in biochar, such as carboxylate and hydroxyl, had a charge that was dependent on the pH level of the solution [45, 57]. These groups became protonated and positively charged at low pH values between 3 and 7. However,

as the pH increased, they became deprotonated [45, 57]. When the pH level fell below the point of zero charge (pH_{pzc}), which was 12 for MgO [8], the surface of biochar became positively charged. This positive charge facilitated the attraction of anionic phosphorus through the process of electrostatic repulsion [45, 57]. Additionally, the dominant type of phosphorus present at a high pH of 7.21 was $H_2PO_4^-$, which easily attached to the adsorption sites. This trend aligned with the findings of previous studies reported in the literature [58-60]. Based on the findings in Figure 4d, it was observed that a higher amount of biochar decreased the PO_4^{3-} adsorption capacity, while a higher PO_4^{3-} initial concentration led to a higher PO_4^{3-} adsorption capacity. This trend was like the one observed in the adsorption of ammonium ions. The two main factors affecting the removal were the initial adsorbate concentration and the adsorbent mass. The chosen model was evaluated for its agreement with the results, and an optimal solution was calculated. This solution involved a pH of 6, a biochar dosage of 0.12 g, an N:P ratio of 1.25, an NH_4^+ concentration of 75 mg/L, and a PO_4^{3-} concentration of 60 mg/L. The desirability of this optimized solution was 0.740, which was close to 1. This suggests that the chosen parameters are suitable for achieving effective removal of ammonium ions and PO_4^{3-}.

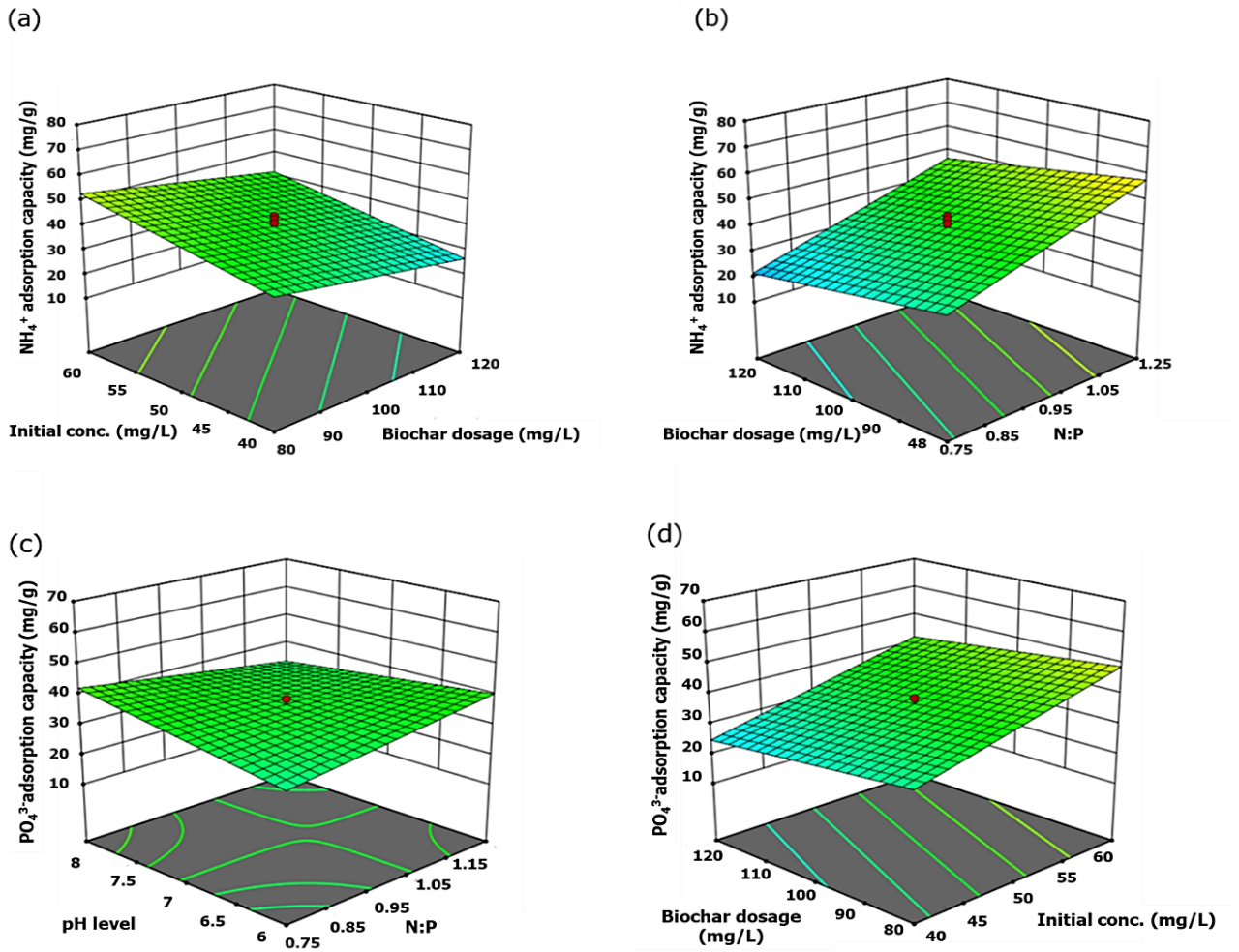

Figure 4 Response surface plots for NH_4^+ adsorption (mg/g) with respect to (a) initial concentration (mg/L) and biochar dosage (mg/L), (b) N:P ratio and initial concentration (mg/L), and PO_4^{3-} adsorption (mg/g) with respect to (c) N:P ratio and pH, (d) biochar dosage (mg/L) and initial concentration (mg/L).

3.3 Testing optimal condition

Figure 5a illustrates the results obtained from the synthetic wastewater test conducted under optimal conditions, including a biochar dosage of 0.12 g/L, N:P ratio of 1.25, pH of 6, and an initial PO_4^{3-} concentration of 60 mg/L. The NH_4^+ adsorption capacity was found to be close to the predicted (53.92 mg/g) and tested (55.00 mg/g) values. These results are comparable to previous studies reporting NH_4^+ capacity of 58.6 mg/g (using 300 mg Mg-biochar/poplar chips, [61]) and 22 mg/g (using 20% Mg-biochar, [18]). Furthermore, biochar made from orange peel, pineapple peel, and dragon fruit peel showed a maximum NH_4^+-N adsorption capacity of 4.71 mg/g, 5.60 mg/g, and 2.65 mg/g, respectively, as reported by Hu et al. [62]. Additionally, Xu et al. [63] investigated the NH_4^+ adsorption capacities of biochar produced from straw, wood chips, reed, and eggshells, which had a maximum NH_4^+-N adsorption capacity of 4.2 mg/g, 3.3 mg/g, 3.2 mg/g, and 2.2 mg/g, respectively [63]. The NH_4^+ concentration met the standard (10 mg/L of QCVN 14:2008/BTNMT, Column B) after the adsorption process. Similarly, for PO_4^{3-}, the predicted (45.65 mg/g) and tested (47 mg/g) values were found to be close to each other. The PO_4^{3-} concentration after adsorption also met the standard (6 mg/L of QCVN 14:2008/BTNMT, Column A). In contrast, Cheng et al. [64] reported that the simultaneous adsorption capability of Eupatorium Adenophora biochar was only 1.91 mg/g for ammonium ions and 2.32 mg/g for phosphate ions. These results demonstrate the effectiveness of rice husk biochar impregnated with 10% $MgCl_2.6H_2O$ in removing NH_4^+ and PO_4^{3-} from synthetic wastewater under optimized conditions.

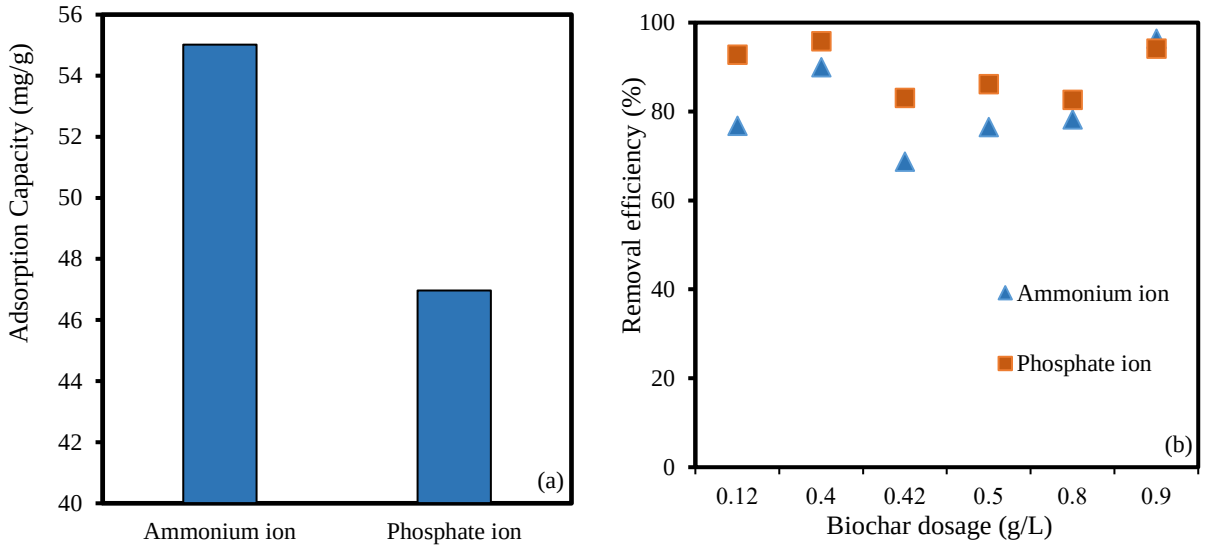

Figure 5 (a) Test in synthetic wastewater (pH 6, N:P ratio of 1.25, biochar dosage of 0.12 g/L, PO_4^{3-} concentration of 60 mg/L, and NH_4^+ concentration of 75 mg/L); (b) Test in domestic wastewater (140 mgNH_4^+/L, 60 mgPO_4^{3-}/L, pH 6, 0.12 – 0.9 g biochar/L)

Figure 5b displays the results obtained from actual domestic wastewater tests, where the initial concentrations of NH_4^+ and PO_4^{3-} were 140 mg/L and 60 mg/L, respectively. Since this was actual wastewater, controlling the conditions was not possible in the same way as the synthetic test. However, the aim of this real wastewater test was to provide practical results for using biochar impregnated with $MgCl_2$. Initially, the NH_4^+ tested value under 0.12 g of the optimized biochar dosage (77%) differed significantly from the predicted value (85.32%) due to the high concentration of NH_4^+ (140 mg/L) and the presence of other inorganic and organic compounds in the actual wastewater. Moreover, co-existing ions in wastewater, such as Al^{3+}, Zn^{2+}, HCO_3^-, CO_3^{2-}, and PO_4^{3-}, could have inhibited the adsorption of NH_4^+ on the Mg-biochar surface [65]. It is worth noting that the optimal adsorption capacity of ammonium by strawberry leaf powder was 7.66 mg/g, 3.93 mg/g, and 6.05 mg/g at 35 °C, 15 °C, and 25 °C, respectively [65]. Consequently, the adsorbent mass had to be increased from the optimized value of 0.12 g to 0.9 g to meet the standard (10 mg/L of QCVN 14:2008/BTNMT, Column B). The NH_4^+ concentration in the treated wastewater with 0.9 g biochar dosage finally met the standard. On the other hand, for PO_4^{3-}, the actual values under 0.12 g biochar dosage (93%) were close to the predicted values (88%), and the PO_4^{3-} concentration after adsorption also met the standard.

4. Conclusions

To enhance the adsorption capacity of rice husk biochar, it was impregnated with 10% $MgCl_2.6H_2O$, which resulted in a surface that was rough and porous. The central composite design model was used to identify the optimal conditions for removing NH_4^+ and PO_4^{3-}. The results from the synthetic wastewater tests were consistent with the model. However, when tested with real wastewater, there were slight differences from the model. Under the optimized conditions of a biochar dosage of 0.12 g/L, N:P ratio of 1.25, pH of 6, and an initial NH_4^+ concentration of 75 mg/L, the NH_4^+ adsorption capacity was 55 mg/g, while that of PO_4^{3-} was 47 mg/g. Despite this, the actual wastewater test did not meet the standard for final NH_4^+ concentration (QCVN 14:2008/BTNMT, Column B), whereas PO_4^{3-} exhibited favorable performance and was in compliance with the standard. In short, while the impregnated biochar showed promising results, further optimization may be required for removing NH_4^+ from real wastewater.

5. Acknowledgements

We acknowledge the support of time and facilities from Ho Chi Minh City University of Technology (HCMUT), VNU-HCM for this study.

6. References

[1] Balat M, Ayar G. Biomass energy in the world, use of biomass and potential trends. Energy Sources. 2005;27(10):931-40.
[2] Canavarro V, Alves JL, Rangel B. Coffee powder reused as a composite material. In: Silva L, editor. Materials Design and Applications. Cham: Springer International Publishing; 2017. p. 113-23.
[3] Nguyen HTQ, Le TK, Nguyen KM. Agricultural residues biomass potential and applying efficiency for household scale biochar production in Go Cong Tay, Tien Giang province. Science & Technology Development Journal - Science of The Earth & Environment. 2017;1(M1):68-78.
[4] Romic M, Romic D. Heavy metals distribution in agricultural topsoils in urban area. Env Geol. 2003;43(7):795-805.
[5] Jaramillo MF, Restrepo I. Wastewater reuse in agriculture: A review about its limitations and benefits. Sustainability. 2017;9(10):1734.
[6] Nguyen TT, Nguyen HN, Nguyen TQA, Phan PT, Nguyen NH. Emission and management for rice husk ash in An Giang Province, Viet Nam. J Viet Env. 2019;11(1):21-6.
[7] Yu-Fong H, Shang-Lien L. 19 - Utilization of rice hull and straw. In: Bao J, editor. Rice Chemistry and Technology. 4th ed. Cambridge: Elsevier; 2019. p. 627-61.

[8] Yin Q, Zhang B, Wang R, Zhao Z. Biochar as an adsorbent for inorganic nitrogen and phosphorus removal from water: a review. Environ Sci Pollut Res. 2017;24(34):26297-309.
[9] Rufí-Salís M, Calvo MJ, Petit-Boix A, Villalba G, Gabarrell X. Exploring nutrient recovery from hydroponics in urban agriculture: an environmental assessment. Resour Conserv Recycl. 2020;155:104683.
[10] Sun D, Hale L, Kar G, Soolanayakanahally R, Adl S. Phosphorus recovery and reuse by pyrolysis: applications for agriculture and environment. Chemosphere. 2018;194:682-91.
[11] Deem LM, Crow SE. Biochar. Reference Module in Earth Systems and Environmental Sciences. Amsterdam: Elsevier; 2017.
[12] Rawat J, Saxena J, Sanwal P. Biochar: a sustainable approach for improving plant growth and soil properties. In: Abrol V, Sharma P, editors. Biochar-an imperative amendment for soil and the environment. London: IntechOpen; 2019. p. 1-17.
[13] Le VG, Vo DVN, Nguyen NH, Shih YJ, Vu CT, Liao CH, et al. Struvite recovery from swine wastewater using fluidized-bed homogeneous granulation process. J Environ Chem Eng. 2021;9(3):105019.
[14] Le VG, Vo DVN, Vu CT, Bui XT, Shih YJ, Huang YH. Applying a novel sequential double-column fluidized bed crystallization process to the recovery of nitrogen, phosphorus, and potassium from swine wastewater. ACS EST Water. 2021;1(3):707-18.
[15] McCarty PL, Bae J, Kim J. Domestic wastewater treatment as a net energy producer–can this be achieved?. Environ Sci Technol. 2011;45:7100-6.
[16] Vazquez-Montiel O, Horan NJ, Mara DD. Management of domestic wastewater for reuse in irrigation. Water Sci Technol. 1996;33(10-11):355-62.
[17] Vu CT, Wu T. Magnetic porous NiLa-Layered double oxides (LDOs) with improved phosphate adsorption and antibacterial activity for treatment of secondary effluent. Water Res. 2020;175:115679.
[18] Li R, Wang JJ, Zhou B, Zhang Z, Liu S, Lei S, et al. Simultaneous capture removal of phosphate, ammonium and organic substances by MgO impregnated biochar and its potential use in swine wastewater treatment. J Clean Prod. 2017;147:96-107.
[19] Xu K, Lin F, Dou X, Zheng M, Tan W, Wang C. Recovery of ammonium and phosphate from urine as value-added fertilizer using wood waste biochar loaded with magnesium oxides. J Clean Prod. 2018;187:205-14.
[20] Le VG, Vu CT, Shih YJ, Bui XT, Liao CH, Huang YH. Phosphorus and potassium recovery from human urine using a fluidized bed homogeneous crystallization (FBHC) process. Chem Eng J. 2020;384:123282.
[21] Vu CT, Wu T. Engineered multifunctional sand for enhanced removal of stormwater runoff contaminants in fixed-bed column systems. Chemosphere. 2019;224:852-61.
[22] Le VG, Vu CT, Shih YJ, Huang YH. Highly efficient recovery of ruthenium from integrated circuit (IC) manufacturing wastewater by Al reduction and cementation. RSC Adv. 2019;9:25303-8.
[23] Phan PT, Nguyen TT, Nguyen NH, Padungthon S. Triamine-bearing activated rice husk ash as an advanced functional material for nitrate removal from aqueous solution. Water Sci Technol. 2019;79(5):850-6.
[24] Phan PT, Nguyen TA, Nguyen NH, Nguyen TT. Modelling approach to nitrate adsorption on triamine-bearing activated rice husk ash. Eng Appl Sci Res 2020;47(2):190-7.
[25] Oldfield TL, Sikirica N, Mondini C, López G, Kuikman PJ, Holden NM. Biochar, compost and biochar-compost blend as options to recover nutrients and sequester carbon. J Environ Manage. 2018;218:465-76.
[26] Yang H, Ye S, Zeng Z, Zeng G, Tan X, Xiao R, et al. Utilization of biochar for resource recovery from water: a review. Chem Eng J. 2020;397:125502.
[27] Thuy NT, Van TDL, Hoan NX, Son LTB, Mai TTN, Thanh DV, et al. Study on the removal of ammonia in wastewater using adsorbent prepared from rice hull with magnesium oxide modification. Viet J Sci Technol. 2020;58(3A):113-23.
[28] Di Capua F, de Sario S, Ferraro A, Petrella A, Race M, Pirozzi F, et al. Phosphorous removal and recovery from urban wastewater: current practices and new directions. Sci Total Environ. 2022;823:153750.
[29] Shakoor MB, Ye ZL, Chen S. Engineered biochars for recovering phosphate and ammonium from wastewater: a review. Sci Total Environ. 2021;779:146240.
[30] Houlton BZ, Almaraz M, Aneja V, Austin AT, Bai E, Cassman KG, et al. A world of co-benefits: Solving the global nitrogen challenge. Earths Future. 2019;7(8):865-72.
[31] Ashenafi N, Mezgebe AG, Leka E. Optimization of amount of spices, roasting temperature and time for field pea (PisumSativum) Shiro flour using response surface methodology. Appl Food Res. 2023;3(1):100257.
[32] Moradi M, Fazlzadehdavil M, Pirsaheb M, Mansouri Y, Khosravi T, Sharafi K. Response surface methodology (RSM) and its application for optimization of ammonium ions removal from aqueous solutions by pumice as a natural and low cost adsorbent. Arch Environ Prot. 2016;42(2):33-43.
[33] Bezerra MA, Santelli RE, Oliveira EP, Villar LS, Escaleira LA. Response surface methodology (RSM) as a tool for optimization in analytical chemistry. Talanta. 2008;76(5):965-77.
[34] Bae IK, Ham HM, Jeong MH, Kim DH, Kim HJ. Simultaneous determination of 15 phenolic compounds and caffeine in teas and mate using RP-HPLC/UV detection: method development and optimization of extraction process. Food Chem. 2015;172:469-75.
[35] Manojkumar N, Muthukumaran C, Sharmila G. A comprehensive review on the application of response surface methodology for optimization of biodiesel production using different oil sources. J King Saud Univ Eng Sci. 2022;34(3):198-208.
[36] Sirichan T, Kijpatanasilp I, Asadatorn N, Assatarakul K. Optimization of ultrasound extraction of functional compound from makiang seed by response surface methodology and antimicrobial activity of optimized extract with its application in orange juice. Ultrason Sonochem. 2022;83:105916.
[37] Yang Y, Li X, Gu Y, Lin H, Jie B, Zhang Q, et al. Adsorption property of fluoride in water by metal organic framework: optimization of the process by response surface methodology technique. Surf Interfaces. 2022;28:101649.
[38] Nguyen VT, Vo TD, Nguyen TB, Dat ND, Huu BT, Nguyen XC, et al. Adsorption of norfloxacin from aqueous solution on biochar derived from spent coffee ground: master variables and response surface method optimized adsorption process. Chemosphere. 2022;288(P2):132577.
[39] Jiang C, Yue F, Li C, Zhou S, Zheng L. Polyethyleneimine-modified lobster shell biochar for the efficient removal of copper ions in aqueous solution: response surface method optimization and adsorption mechanism. J Environ Chem Eng. 2022;10(6):108996.
[40] Visser W, Hoc JM. Chapter 3.3 - Expert software design strategies. In: Hoc JM, Green TRG, Samurcay R, Gilmore DJ, editors. Psychology of programming. London: Elsevier; 1990. p. 235-49.

[41] Alben KT. Books and Software: Design, analyze, and optimize with Design-Expert. Anal Chem. 2002;74(7):222-3.
[42] Pham H. Springer handbook of engineering statistics. Germany: Springer; 2006.
[43] Rozainee M, Ngo SP, Salema A, Tan KG, Ariffin M, Zainura Z. Effect of fluidising velocity on the combustion of rice husk in a bench-scale fluidised bed combustor for the production of amorphous rice husk ash. Bioresour Technol. 2008;99(4):703-13.
[44] Tran VS, Ngo HH, Guo W, Zhang J, Liang S, Ton-That C, et al. Typical low cost biosorbents for adsorptive removal of specific organic pollutants from water. Bioresour Technol. 2015;182:353-63.
[45] Luo D, Wang L, Nan H, Cao Y, Wang H, Kumar TV, et al. Phosphorus adsorption by functionalized biochar: a review. Environ Chem Lett. 2023;21:497-524.
[46] Zhang M, Song G, Gelardi DL, Huang L, Khan E, Masek O, et al. Evaluating biochar and its modifications for the removal of ammonium, nitrate, and phosphate in water. Water Res. 2020;186:116303.
[47] Lehmann J, Joseph S. Biochar for Environmental Management. London: Earthscan; 2015.
[48] Spokas KA. Review of the stability of biochar in soils: predictability of O:C molar ratios. Carbon Manag. 2010;1(2):289-303.
[49] Cross A, Sohi SP. A method for screening the relative long-term stability of biochar. GCB Bioenergy. 2013;5(2):215-20.
[50] Wang S, Wang Q, Hu Y, Xu S, He Z, Ji H. Study on the synergistic co-pyrolysis behaviors of mixed rice husk and two types of seaweed by a combined TG-FTIR technique. J Anal Appl Pyrolysis. 2015;114:109-18.
[51] Chen D, Zhou J, Zhang Q. Effects of torrefaction on the pyrolysis behavior and bio-oil properties of rice husk by using TG-FTIR and Py-GC/MS. Energy Fuels. 2014;28(9):5857-63.
[52] Yin Q, Si L, Wang R, Zhao Z, Li H, Wen Z. DFT study on the effect of functional groups of carbonaceous surface on ammonium adsorption from water. Chemosphere. 2022;287(P3):132294.
[53] Liu P, Zhang A, Liu Y, Liu Z, Liu X, Yang L, et al. Adsorption mechanism of high-concentration ammonium by chinese natural zeolite with experimental optimization and theoretical computation. Water 2022;14(15):2413.
[54] Del Nero M, Galindo C, Barillon R, Halter E, Made B. Surface reactivity of alpha-Al_2O_3 and mechanisms of phosphate sorption: *In situ* ATR-FTIR spectroscopy and zeta potential studies. J Colloid Interface Sci. 2010;342(2):437-44.
[55] Li R, Wang JJ, Zhou B, Awasthi MK, Ali A, Zhang Z, et al. Enhancing phosphate adsorption by Mg/Al layered double hydroxide functionalized biochar with different Mg/Al ratios. Sci Total Environ. 2016;559:121-9.
[56] He Q, Li X, Ren Y. Analysis of the simultaneous adsorption mechanism of ammonium and phosphate on magnesium-modified biochar and the slow release effect of fertiliser. Biochar. 2022;4:1-16.
[57] Hou L, Liang Q, Wang F. Mechanisms that control the adsorption-desorption behavior of phosphate on magnetite nanoparticles: the role of particle size and surface chemistry characteristics. RSC Adv. 2020;10:2378-88.
[58] Wang Z, Shen D, Shen F, Li T. Phosphate adsorption on lanthanum loaded biochar. Chemosphere. 2016;150:1-7.
[59] Li J, Li B, Huang H, Zhao N, Zhang M, Cao L. Investigation into lanthanum-coated biochar obtained from urban dewatered sewage sludge for enhanced phosphate adsorption. Sci Total Environ. 2020;714:136839.
[60] Cui Q, Xu J, Wang W, Tan L, Cui Y, Wang T, et al. Phosphorus recovery by core-shell gamma-Al_2O_3/Fe_3O_4 biochar composite from aqueous phosphate solutions. Sci Total Environ. 2020;729:138892.
[61] Yin Q, Liu M, Ren H. Removal of ammonium and phosphate from water by Mg-modified biochar: Influence of Mg pretreatment and pyrolysis temperature. BioRes. 2019;14(3):6203-18.
[62] Hu X, Zhang X, Ngo HH, Guo W, Wen H, Li C, et al. Comparison study on the ammonium adsorption of the biochars derived from different kinds of fruit peel. Sci Total Environ. 2020;707:135544.
[63] Xu K, Zhang C, Dou X, Ma W, Wang C. Optimizing the modification of wood waste biochar via metal oxides to remove and recover phosphate from human urine. Environ Geochem Health. 2019;41(4):1767-76.
[64] Cheng N, Wang B, Feng Q, Zhang X, Chen M. Co-adsorption performance and mechanism of nitrogen and phosphorus onto eupatorium adenophorum biochar in water. Bioresour Technol. 2021;340:125696.
[65] Liu H, Dong Y, Wang H, Liu Y. Ammonium adsorption from aqueous solutions by strawberry leaf powder: Equilibrium, kinetics and effects of coexisting ions. Desalination. 2010;263(1-3):70-5.